

Estimation of Contraction Scour in Riverbed Using SERF

Jianhua Jiang¹; Neil K. Ganju²; and Ashish J. Mehta, M.ASCE³

Abstract: Contraction scour in a firm-clay estuarine riverbed is estimated at an oil-unloading terminal at the Port of Haldia in India, where a scour hole attained a maximum depth greater than 5 m relative to the original bottom. A linear equation for the erosion flux as a function of the excess bed shear stress was semicalibrated in a rotating-cylinder device called SERF (Simulator of Erosion Rate Function) and coupled to a hydrodynamic code to simulate the hole as a clear-water scour process. SERF, whose essential design is based on previous such devices, additionally included a load cell for in situ and rapid measurement of the eroded sediment mass. Based on SERF's performance and the degree of comparison between measured and simulated hole geometry, it appears that this device holds promise as a simple tool for prediction of scour in firm-clay beds.

DOI: 10.1061/(ASCE)0733-950X(2004)130:4(215)

CE Database subject headings: Scour; River beds; Contraction; India; Clays; Harbors; Erosion.

Introduction

At a riverbed composed of an overconsolidated clay, flow contraction scour near a newly placed structure can at times be so slow that a noticeable hole may not appear for months to years. In anticipation of such an eventuality, however, it behooves the engineer to incorporate calculations that address the issue of whether a hole will develop, especially if it is likely to undermine the structure itself. A problem at an oil terminal for crude from 40,000 dead weight tons (DWT) tankers at the Port of Haldia on the Hooghly River estuary in India (Fig. 1) offered the opportunity to estimate hole dimensions using a laboratory testing device coupled with numerical modeling. The outcome of this analysis is summarized here.

Scour Problem

At the Haldia concrete-pile terminal, a noticeable scour hole was detected in a bottom survey taken in 1979, after oil tankers began to dock regularly. Docking apparently accentuated contraction scour adjacent to the terminal by generating bottom-directed currents under the keel (Engineers India Ltd. 1980). A survey taken about 40 months later found that the hole had attained a maximum depth greater than 5 m below the mean depth of ~10 m in

the region (Fig. 2), and its horizontal extent was greater than twice that of the vessel keel. As the pile foundation was potentially threatened by the hole, in subsequent years the question arose, of retrofitting the terminal or rebuilding a new one at a nearby more stable site and was the motivation for the present analysis.

Even though semidiurnal tide penetrates the site from the Bay of Bengal, a strong ebb-dominated current due to river outflow led to an off-center, downstream orientation of the hole with respect to the terminal (Fig. 2). The outflow averages between 1,400 and 2,300 m³·s⁻¹ during the monsoon months (June–September), but is an order of magnitude lower during the dry period, especially March–May. Obstruction to flow due to the terminal causeway and the piles led to a severe deflection of the ebb flow, and the mean speed in the area of high scour increased from about 0.90 to 1.1 m·s⁻¹. Under such a current, and given a low rate of supply of sediment in the river with concentrations on the order of 0.1–0.3 kg·m⁻³ only, the effect of flow contraction could be treated as a case of clear-water scour [for example, Chen (2002)].

The bed consisted of a firm blue clay with a wet bulk density $\rho_b \approx 1,800 \text{ kg}\cdot\text{m}^{-3}$, vane shear strength on the order of 10² kPa, and a critical shear stress for erosion, τ_c , in the range of 3–5 Pa measured in flume tests (Engineers India Ltd. 1980). The latter value is as much as two orders of magnitude greater than τ_c for typical fresh clay deposits (Mehta and Parchure 2000).

Among the empirical erosion flux functions available to model the rate of scour of such a bed, we chose the commonly used linear equation

$$\varepsilon = z_1 \frac{dC_1}{dt} = \varepsilon_N (\tau_b - \tau_c) \quad (1)$$

where ε =erosion flux (dry sediment mass per unit area per unit time); z_1 =characteristic bottom water layer height; C_1 =total suspended solids concentration within z_1 ; t =time; ε_N =erosion flux constant; and τ_b =bed shear stress. Inasmuch as ε_N was unknown, to estimate it we constructed a small rotating-cylinder device called the Simulator of Erosion Rate Function (SERF). Since it proved to be impractical to procure the original clay, we tested

¹Coastal Engineer, ASL Environmental Sciences, Inc., 1986 Mills Rd., Sidney BC, Canada V8L 5Y3.

²Hydraulic Engineer, U.S. Geological Survey, 6000 J St., Sacramento, CA 95819.

³Professor, Dept. of Civil and Coastal Engineering, Univ. of Florida, Gainesville, FL 32611.

Note. Discussion open until December 1, 2004. Separate discussions must be submitted for individual papers. To extend the closing date by one month, a written request must be filed with the ASCE Managing Editor. The manuscript for this technical note was submitted for review and possible publication on February 3, 2003; approved on December 9, 2003. This technical note is part of the *Journal of Waterway, Port, Coastal, and Ocean Engineering*, Vol. 130, No. 4, July 1, 2004. ©ASCE, ISSN 0733-950X/2004/4-215–218/\$18.00.

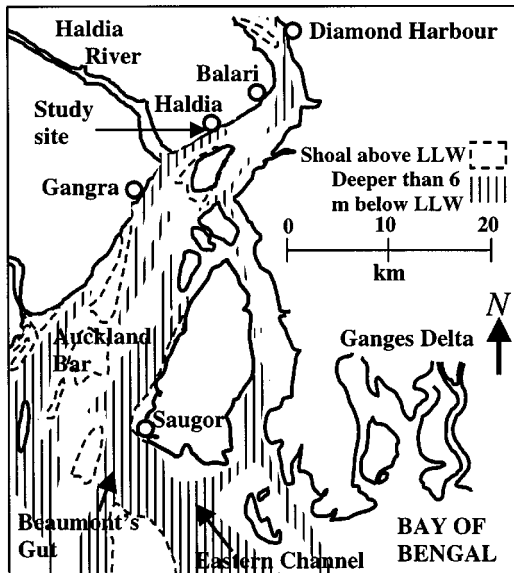


Fig. 1. Study site near Port of Haldia, India

potter's clay beds as surrogates (Barry 2003). Three highly plastic montmorillonitic clays, identified by Bennett Pottery Supply Inc. of Orlando, Florida, as clay nos. 10, 20, and 75, were chosen on the basis of their similarity to the clay from the site in terms of high bulk density (for all three, $\sim 2,000 \text{ kg}\cdot\text{m}^{-3}$) and vane shear strength ($\sim 10^2 \text{ kPa}$). The dispersed, that is, deflocculated grain size of these clays was nominally $1 \mu\text{m}$. They had been pretreated with chemicals to impart different colors and textures, due to which the clays were in a flocculated state.

Scour Simulation

SERF, sketched in Fig. 3, is similar in design to a device described by Arulanandan et al. (1975). The latter device has been used extensively for testing of the erodibility of clays with variable composition and pore water chemistry by Kandiah (1974). SERF has the advantage of using small clay samples that typically require a high-flow-speed facility for erosion tests. A requirement is that the sample be of strength sufficient to stand up on its own without deformation due to its own weight. After carefully molding a cylindrical sample of 76 mm diameter around a shaft-and-disc mandrel, the assembly is suspended inside an acrylic outer cylinder of 102 mm internal diameter from a load cell and submerged in water (confined within the 26 mm annular gap) acting as the eroding fluid. The outer cylinder is then spun at

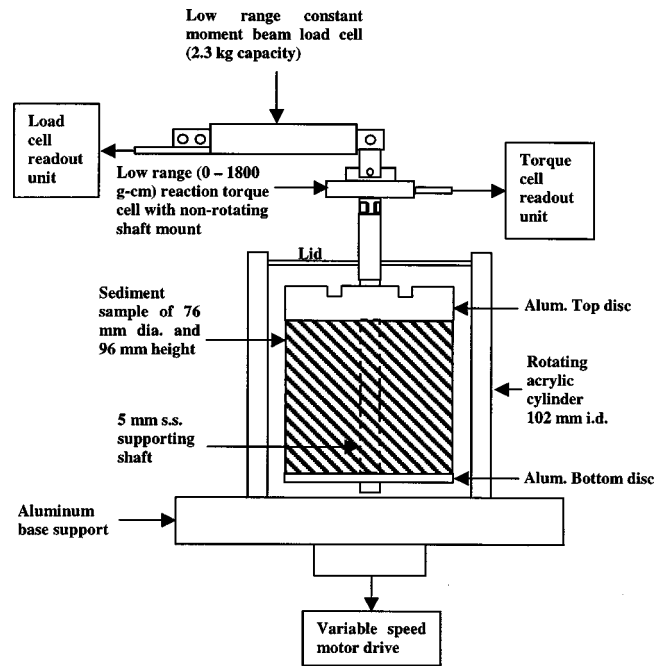


Fig. 3. Elevation view of SERF (not drawn to scale)

a selected rpm (1,600 maximum), which yields the desired shear stress on the sample surface from the torque measured by a strain-gauge cell.

After a suitable duration (up to 15 min), the device is stopped and the loss of suspended clay mass due to erosion at its cylindrical surface is obtained from the load-cell readout. The erosion flux is then calculated from this loss. This arrangement obviates the time-consuming requirement, in earlier such devices, to remove the sample and weigh it apart from the device. SERF operates at a considerably higher rpm (~ 800 minimum at a Reynolds number of 10^5) than the rpm (~ 150) at which Taylor vortices within such annular devices destabilize the flow (Schlichting 1968). Consequently, the stress field is believed to be acceptably uniform over the cylindrical bed surface at a constant rpm.

Sample outputs of ϵ versus τ_b are plotted in Fig. 4, and values of ϵ_N and τ_c derived from the respective best-fit straight lines [per Eq. (1)] from 15 tests are given in Table 1. Small aliquots of water had to be added to the original clays to vary sample density (1,435 to $1,963 \text{ kg}\cdot\text{m}^{-3}$). From the τ_c values we observe that erodibility increased from clay nos. 10 to 75. In general, for a given clay bed, as the density increased τ_c increased while ϵ_N decreased, as seen for example from test nos. 9, 10, 11, and 12 for

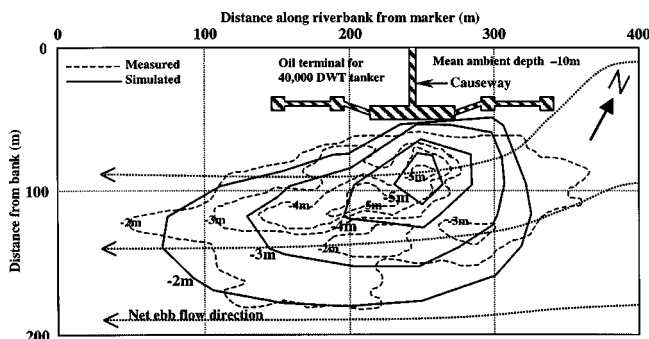


Fig. 2. Measured and simulated scour holes near oil terminal

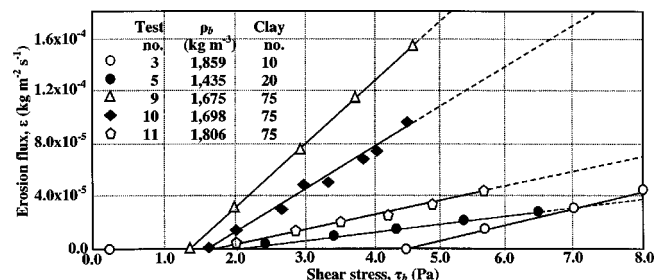


Fig. 4. Example plots of erosion flux versus bed-shear stress

Table 1. Erosion Flux Parameters Obtained from SERF

Test number	Clay number	Pore-water salinity (%)	Bulk density, ρ_b ($\text{kg}\cdot\text{m}^{-3}$)	Erosion flux parameters	
				ε_N ($\text{kg}\cdot\text{N}^{-1}\cdot\text{s}^{-1}$)	τ_c (Pa)
1	10	0	1,665	5.0×10^{-5}	3.1
2	10	0	1,710	1.9×10^{-5}	3.4
3	10	0	1,859	1.2×10^{-5}	4.5
4	10	0	1,928	1.0×10^{-5}	4.7
5	20	0	1,435	3.9×10^{-5}	1.9
6	20	0	1,537	1.2×10^{-5}	2.8
7	20	0	1,721	7.7×10^{-6}	3.0
8	20	0	1,905	7.1×10^{-6}	3.0
9	75	0	1,675	4.8×10^{-5}	1.4
10	75	0	1,698	3.2×10^{-5}	1.7
11	75	0	1,806	1.1×10^{-5}	1.8
12	75	0	1,963	9.9×10^{-6}	1.9
13	10	35	1,928	1.7×10^{-5}	0.6
14	20	35	1,894	4.4×10^{-5}	1.6
15	75	35	1,940	5.1×10^{-5}	3.3

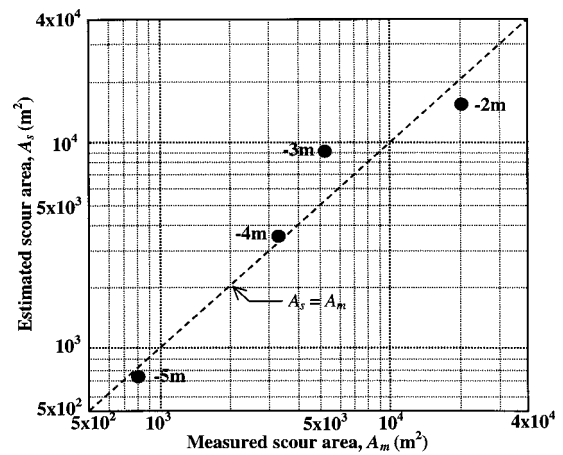
clay no. 75 in fresh water as eroding fluid. This trend is consistent with previous results on clay bed erosion (Arulananand et al. 1975).

For gaining an understanding of the effect of high salinity on erosion, in the last three tests the clay was equilibrated for several days with an NaCl solution in sufficient quantity to yield a pore-fluid salinity of about 35%. In general, bed weakening due to the formation of flocs with a more open structure than in fresh water is suggested. Compare for instance test no. 4 with no. 13, both using clay no. 10 and an initial bulk density of $1,928\text{ kg}\cdot\text{m}^{-3}$. We note that τ_c decreased from 4.7 to 0.6 Pa as ε_N increased from 1.0×10^{-5} to $1.7 \times 10^{-5}\text{ kg}\cdot\text{N}^{-1}\cdot\text{s}^{-1}$. A similar trend is observed for clay no. 20, when test no. 8 is compared with no. 14. Finally, for clay no. 75, when test no. 12 is compared with no. 15 we observe an increase in the erosion rate, from 9.9×10^{-6} to $5.1 \times 10^{-5}\text{ kg}\cdot\text{N}^{-1}\cdot\text{s}^{-1}$, which is consistent with the other two comparisons, but unlike those cases, τ_c increased from 1.9 to 3.3 Pa. Until further exploratory tests are carried out, we attribute this seeming discrepancy to the effect of salinity on that particular clay.

Inasmuch as the sediment was flocculated in all tests, we chose the bed in test no. 3 (without NaCl) having a bulk density of $1,859\text{ kg}\cdot\text{m}^{-3}$, $\tau_c=4.5\text{ Pa}$ (which was within the range of τ_c 3–5 Pa for the clay from the site, as noted), and $\varepsilon_N=1.2 \times 10^{-5}\text{ kg}\cdot\text{N}^{-1}\cdot\text{s}^{-1}$ as representing the prototype bed and simulated the scour hole as follows. A 3D shallow-water hydrodynamic code based on the numerical scheme of Casulli and Cheng (1992) was used in its nonstratified flow mode to simulate the river reach from 2.25 km upstream to the same distance downstream of the terminal. The development of this model, its calibration and validation, and the requisite flow boundary conditions used in the present simulation are described by Jiang (1999). The use of the vertical, σ -transformed coordinate in the model allowed the selection of $z_1=0.05h$, where h is the instantaneous local depth. The bed shear stress vector τ_b was then obtained from

$$\tau_b = C_D \rho |\mathbf{U}_1| \mathbf{U}_1 \quad (2)$$

$$C_D = \left[\frac{\kappa}{\ln(z_1/z_0)} \right]^2 \quad (3)$$

**Fig. 5.** Measured and estimated scour hole planform areas at different depths

where \mathbf{U}_1 =horizontal velocity vector at height z_1 ; ρ =water density (nominally $1,000\text{ kg}\cdot\text{m}^{-3}$); C_D =bottom drag coefficient; κ =von Kármán constant ($=0.4$); and z_0 =effective bottom roughness height. A value of $z_0=0.1\text{ mm}$ yielded current velocities that reasonably agreed with measurements (Engineers India Ltd. 1980). Based on this agreement, simulation was carried out for the mean flow condition near the terminal, with a river discharge of $750\text{ m}^3\cdot\text{s}^{-1}$.

The stress field per Eqs. (2) and (3) along with Eq. (1) allowed the progression of scour to be determined in an approximate way without the use of a sediment transport code [for example, Jiang (1999); Jiang and Mehta (2000)] required for higher accuracy. The incremental scour depth Δz was accordingly calculated as

$$\Delta z = \frac{\varepsilon_N(\tau_b - \tau_c)}{\rho_b} \Delta t \quad (4)$$

where Δt =time increment. For computational stability a 5 s increment was adopted, and the local water depth was updated after each time increment.

Results obtained after 12 months of simulation are shown in Fig. 5, in which the measured planform area, A_m , at different scour depths from Fig. 2 is compared with model-derived estimates, A_e . Despite evident discrepancies, particularly at -3 m depth at which the estimate is only 60% of the measured value, the general appearance of the simulated hole is akin to what occurred at the site.

It is noteworthy that hole simulations for times longer than 12 months indicated that the hole had practically reached its equilibrium dimensions in about a year. This in turn suggests that the measured hole at 40 months had probably attained that size months earlier.

Concluding Comments

One can expect that inclusion of in situ bed erosion flux data as well as seasonal variability of flow would improve prediction of hole dimensions. Nonetheless, we found SERF to be a useful tool for rapid measurement of erosion of stiff clay beds. A future de-

sign modification could include the ability to achieve shear stresses higher than the 8 Pa (maximum) we were able to apply.

Notation

The following symbols are used in this technical note:

- A_e = estimated planform scour area;
- A_m = measured planform scour area;
- C_D = bottom drag coefficient;
- C_1 = near-bed value of suspended sediment concentration;
- h = instantaneous local depth;
- rpm = revolutions per minute;
- t = time;
- \mathbf{U}_1 = horizontal velocity vector at height z_1 ;
- z_1 = bottom water layer height;
- Δt = time increment;
- Δz = incremental scour depth;
- ε = erosion flux;
- ε_N = erosion flux constant;
- κ = von Kármán constant;
- ρ = water density;
- ρ_b = wet bulk density of sediment;
- σ = transformed vertical coordinate;
- $\boldsymbol{\tau}_b$ = bed shear stress vector;
- τ_b = bed shear stress; and
- τ_c = critical shear stress for erosion.

References

- Arulanandan, K., Krone, R. B., and Loganathan, P. (1975). "Pore and eroding fluid influences on surface erosion on soil." *J. Geotech. Eng. Div., Am. Soc. Civ. Eng.*, 101(1), 51–66.
- Barry, K. M. (2003). "The effect of clay particles in pore water on the erosion of sand." PhD thesis, Univ. of Florida, Gainesville, Fla.
- Casulli, V., and Cheng, R. T. (1992). "Semi-implicit finite-difference method for three-dimensional shallow water flow." *Int. J. Numer. Methods Fluids*, 15(6), 629–648.
- Chen, H.-C. (2002). "Numerical simulation of scour around complex piers in cohesive soil." *Proc., 1st Int. Conf. on Scour of Foundations*, Texas A&M Univ., College Station, Tex., 14–33.
- Engineers India Ltd. (1980). "Technical feasibility report—Second oil unloading terminal for Haldia." Vol. II, *Rep. Prepared for the Ministry of Shipping and Transport, Government of India*, New Delhi, India.
- Jiang, J. (1999). "An examination of estuarine lutocline dynamics." PhD thesis, Univ. of Florida, Gainesville, Fla.
- Jiang, J., and Mehta, A. J. (2000). "Lutocline behavior in high-concentration estuary." *J. Hydraul. Eng.*, 126(6), 324–328.
- Kandiah, A. (1974). "Fundamental aspects of surface erosion of cohesive soils." PhD thesis, Univ. of California, Davis, Calif.
- Mehta, A. J., and Parchure, T. M. (2000). "Surface erosion of fine-grained sediment revisited." *Muddy coast dynamics and resource management*, B. W. Flemming, M. T. Delafontaine, and G. Liebezeit, eds., Elsevier, Amsterdam, The Netherlands, 55–74.
- Schlichting, H. (1968). *Boundary-layer theory*, 6th Ed., McGraw-Hill, New York.